Research Square

Preprints are preliminary reports that have not undergone peer review.
They should not be considered conclusive, used to inform clinical practice,
or referenced by the media as validated information.

An update to the critical vaccination threshold for measles herd immunity

Mahmuda Ruma
York University
Elena Aruffo
York University
Alexandra Teslya
Utrecht University
Jane Heffernan
jmhefer@yorku.ca
York University

Research Article

Keywords:

Posted Date: June 30th, 2026

DOI: https://doi.org/10.21203/rs.3.rs-10059899/v1

License: This work is licensed under a Creative Commons Attribution 4.0 International License.
Read Full License

Additional Declarations: No competing interests reported.

An update to the critical vaccination threshold for measles herd immunity

Mahmuda Ruma[1], Elena Aruffo[1], Alexandra Teslya[2], Jane M. Heffernan[1,*]

[1] Modelling Infection and Immunity Lab, Centre for Disease Modelling, Mathematics and Statistics, York University, Toronto, ON, Canada

[2] Julius Center for Health Sciences and Primary Care, University Medical Center Utrecht, Utrecht University, Utrecht, The Netherlands

[*] Correspondence: jmheffer@yorku.ca

1 Abstract

Recent evidence indicates that measles vaccine-induced immunity may wane over time, challenging the classical assumption of lifelong protection. We develop a mathematical model of measles transmission and vaccination that explicitly incorporates waning immunity and derive updated expressions for the critical vaccination threshold (p_c) and control reproduction number (R_c), two cornerstone metrics used to guide public health vaccination policy. We additionally derive equations for outbreak probability and final outbreak size. We apply the model to the 2024-2025 measles outbreak in the Southwestern Ontario Public Health Region, estimating the basic reproduction number (R_0), outbreak peak timing and magnitude, final outbreak size, and the size of the population involved in transmission. Most importantly, our analysis reveals that even extremely slow waning of vaccine-induced immunity – effectively corresponding to lifelong protection – can fundamentally alter herd immunity dynamics. Specifically, we identify realistic parameter regimes in which vaccine-induced herd immunity cannot be achieved, despite high vaccine coverage. Nevertheless, outbreak risk under these conditions may still remain very low. These findings suggest that widely used measles herd immunity thresholds may require re-evaluation in highly vaccinated populations.

2 Introduction

Measles, caused by the measles virus (MeV), is a very contagious childhood disease [1]. Despite the existence of a highly effective vaccine [2], measles cases continue to persist worldwide, causing significant morbidity and mortality [2, 3] . The World Health Organization (WHO) recommends that every child receive two doses of the measles vaccine [4]. Seroconversion following a single dose of vaccine is estimated to be 95% [5]. Vaccine effectiveness has been approximated to be 93-96.7%, and 97-99.7%, after one and two doses [6, 7].

In 2024-2025, measles cases have been reported across Canada [8], a country with relatively high vaccination coverage [9]. While measles infections have been mainly reported in the unvaccinated, individuals with one or two doses have also contracted the disease [8]. Measles cases in vaccinated individuals have been reported previously [10, 11, 12]. A recent study by Bolotin et al. [13] showed that

antibody immunity can decay over time in vaccinated individuals, whereby some susceptibility could be reached approximately 51 years after full immunization.

Assuming lifelong immunity from vaccination, mathematical models have shown that herd immunity can be achieved in populations that maintain vaccine uptake greater than $p_c = 1 - 1/\mathcal{R}_0$, where R_0 is the basic reproduction number and quantifies the infection transmission potential of a disease [14, 15]. Historically, the basic reproduction number for measles has been reported to fall between 12 to 18 [1], though a recent study has identified a much larger range, with median values for different geographic regions lying between 11-16 [16]. Given these values, it is has been widely accepted that a critical vaccination threshold of at least 95% should be the goal to achieve herd immunity across the globe [4].

If measles immunity gained from vaccination wanes, calculations of the critical vaccination threshold p_c must be revisited. Herewithin, we develop and utilize a mathematical model to determine this critical threshold and investigate its dependence on the waning rate of immunity. Further, we investigate the effects of the waning rate on other important calculations related to measles: the probability of an outbreak, and the final size of such an outbreak. Finally, we apply our mathematical model to a measles outbreak in Southwestern Ontario, Canada. The mathematical models employed here are extensions of the well-known Susceptible-Infected-Recovered (SIR) model to include vaccination and the waning and boosting of vaccine-conferred immunity.

3 Model

The model is based on an $SIRVWS$ framework [17, 18, 19, 20] that delineates the population into susceptible individuals, S; individuals who have recovered from infection and are subsequently immune to the pathogen, R; vaccinated individuals with full protection from infection, V; vaccinated individuals in waning stages of immunity, W; infected individuals who were exposed to the pathogen while in the susceptible (S) or waning immunity (W) classes, I and I_W, respectively. The model equations are:

$$\begin{aligned}
S' =& \lambda(1-p) - \beta S(I + GI_W) + k_2 W - dS \\
I' =& \beta S(I + GI_W) - \gamma I - dI \\
I'_W =& \nu(1-q)\beta(I + GI_W)W - \gamma_W I_W - dI_W \\
R' =& \gamma I + \gamma_W I_W - dR \\
V' =& \lambda p - dV - k_1 V + q\nu\beta(I + GI_W)W \\
W' =& k_1 V - \nu\beta(I + GI_W)W - k_2 W - dW
\end{aligned} \tag{1}$$

Table 1 lists the variables and parameters of the system, scaled such that the total population has a value of unity. The model flow diagram is shown in Figure 1.

Model (1) incorporates demographic dynamics such that birth and death processes are balanced, keeping the population size (N) constant. It is assumed that individuals enter the model population upon the age of first measles vaccination ($\approx$ age 1). This occurs at rate $\lambda = dN$ individuals per year. Individuals leave the population at average rate d per year. Upon entrance, a fraction p of individuals are vaccinated and enter the V population, while $1-p$ remain susceptible and proceed to compartment S. Vaccinated individuals can experience waning immunity whereby they proceed to the W class with rate k_1 and then to the S class with rate k_2.

Susceptible individuals (S) can become infected when they come into contact with infectious individuals, after which they move to the fully infected class, I. Upon exposure to the virus, individuals in the waning immunity class can also be infected (and move to the I_W class), but they can also experience a boost in immunity (and move to the V class). We note that fraction q of W individuals will experience a

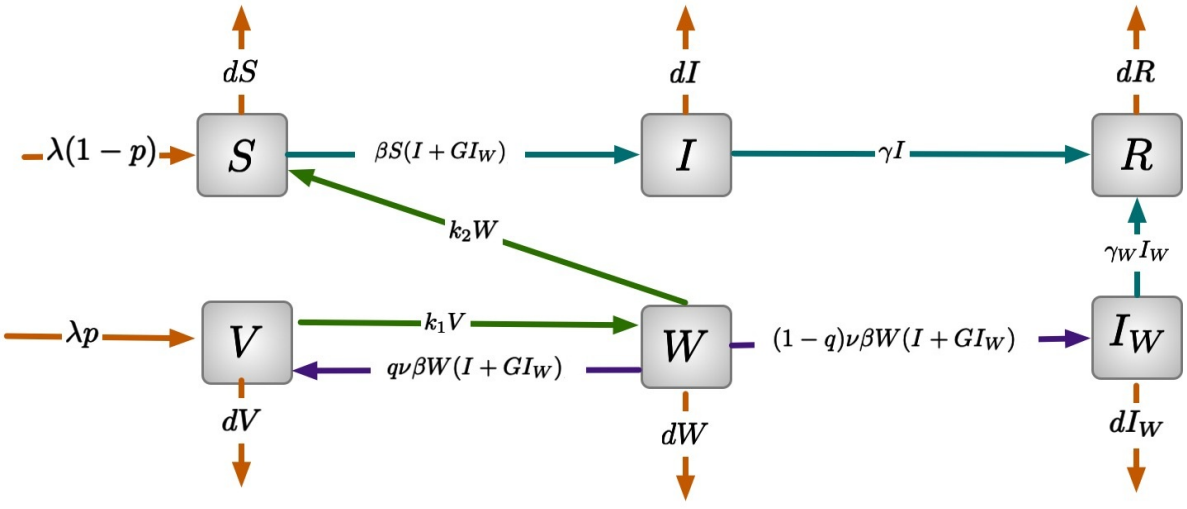


Figure 1: Flow diagram of System (1). Orange arrows are associated with demographics. Green arrows show the path of waning immunity. Purple arrows show the outcomes of exposure of waning immunity W individuals to infection or boosting of immunity. Blue arrows show all other paths and are associated with infection and recovery.

boost in immunity rather than an infection and that this is scaled by a boosting proportionality constant ν which represents the frequency of exposure events that occur to W compared to the rate with which S becomes infected.

We assume that the population mixes homogeneously, meaning that S and W individuals come into contact with infected individuals with frequency-dependent rate $\beta\,(I + GI_W)$, where $0 < G < 1$ represents a reduction in infectiousness of I_W individuals compared to those in the fully infected class, I. On average, infected individuals I and I_W are infected and infectious for $1/\gamma$ and $1/\gamma_W$ time units, respectively, where $1/\gamma \geq 1/\gamma_W$ since I_W individuals can experience milder and shorter infections given their pre-existing immunity at the time of exposure to the virus. Upon recovery, it is assumed that I and I_W infections move to the R class where they will have lifelong protective immunity.

4 Results

4.1 Disease Free Equilibrium

System (1) has a unique disease-free equilibrium (DFE) $E_0 = (S_0, 0, 0, 0, V_0, W_0)$, where

$$\begin{aligned} S_0 &= N\left(1 - p + \frac{pk_1k_2}{(d+k_1)(d+k_2)}\right) \\ V_0 &= N\left(\frac{pd}{d+k_1}\right) \\ W_0 &= N\left(\frac{pdk_1}{(d+k_1)(d+k_2)}\right) \end{aligned} \tag{2}$$

where N is the size of the total population. We note that N is constant when $\lambda = dN$.

Variables	
Name	**Definition**
S	Fully susceptible population
I	Infected population coming from the susceptible class S
I_W	Infected population coming from the waning immunity class W
R	Recovered population that is characterized by the life-long immunity
V	Population with immunity gained after vaccination or immune boosting
W	Population in the immunity waning stage.

Parameters			
Name	**Definition (unit)**	**Value [Interval]**	**Source**
d	Natural death rate (year^{-1})	0.012	[21]
λ	Birth rate (people $\times$ year^{-1})	0.012	$\lambda = dN$
p	Fraction of newborns that were effectively vaccinated (obtained vaccine and gained a level of neutralizing immunity)	[0.7,1]	
$\mathcal{R}_0$	Basic Reproduction Number	[3 , 27]	[16]
β	Infection rate (people $\times$year)$^{-1}$	[34.69, 312.22]	Calculated from $\mathcal{R}_0$ (Eq. (3))
γ	Recovery rate of I (year^{-1})	26	[22]
γ_W	Recovery rate of I_W (year^{-1})	$\gamma_W = a\gamma$, $a \geq 1$	
G	Reduction in infectiousness of I_W	[0 , 1]	
ν	Boosting proportionality constant, or susceptibility of W	[0 , 1]	
q	Fraction of W whose immunity is boosted upon exposure to infection	[0,1]	
k_1	Transition rate from V to W due to waning of immunity (year^{-1})	[0 , 1]	
k_2	Transition rate from W to S due to waning of immunity (year^{-1})	[0 , 1]	

Table 1: Model variables and parameters

4.2 Basic and Control Reproduction Numbers

Using the Next Generation Matrix method [15, 14] the basic and control reproduction numbers of the system are

$$\mathcal{R}_0 = \frac{\beta N}{(\gamma + d)} \tag{3}$$

and

$$\begin{aligned} \mathcal{R}_c &= \mathcal{R}_0 \left[(1-p) + p\tfrac{k_1 k_2}{(d+k_1)(d+k_2)} + Gp\tfrac{(1-q)\nu k_1 d(d+\gamma)}{(d+k_1)(d+k_2)(d+\gamma_W)} \right] \\ &= \mathcal{R}_0 \left[(1-p) + p\tfrac{k_1 k_2}{(d+k_1)(d+k_2)} \right] + \mathcal{R}_0 \left[Gp\tfrac{(1-q)\nu k_1 d(d+\gamma)}{(d+k_1)(d+k_2)(d+\gamma_W)} \right] \\ &= \mathcal{R}_{0,I\to I} + \mathcal{R}_{0,I_W\to I_W} \end{aligned} \tag{4}$$

where type reproduction numbers $\mathcal{R}_{0,I\to I}$ and $\mathcal{R}_{0,I_W\to I_W}$ correspond to the number of new I infecteds that one I infected makes and the number of new I_W infecteds that one I_W infected makes, respectively (see Appendix for details). Note that if G, q or ν are small the latter term makes an insignificant contribution to $\mathcal{R}_c$. Additionally, observe that as waning rates k_1 and k_2 go to zero, $\mathcal{R}_{0,I\to I} \to \mathcal{R}_0(1-p)$ and $\mathcal{R}_{0,I_W\to I_W} \to 0$, and Eq. (4) gives $\mathcal{R}_c \approx (1-p)\mathcal{R}_0$, which corresponds to the case when vaccine-induced immunity does not wane. On the other hand, if immunity wanes quickly (k_1, k_2 large), $\mathcal{R}_c \approx \mathcal{R}_0$, since $\mathcal{R}_{0,I\to I} \to \mathcal{R}_0$ and $\mathcal{R}_{0,I_W\to I_W} \to 0$.

4.3 Critical Vaccination Threshold for Herd Immunity

When $\mathcal{R}_0 > 1$ infectious diseases can spread, but the spread can be limited by vaccination campaigns. The spread can also be halted if herd immunity is achieved. Taking Eq. (4), and letting $p = p_c$ and $R_c = 1$, we find that the critical vaccination uptake threshold p_c necessary to obtain herd immunity is

$$p_c = \left(1 - \frac{1}{\mathcal{R}_0}\right) \frac{(d+k_1)(d+k_2)(d+\gamma_W)}{d[(d+k_1+k_2)(d+\gamma_W) - Gk_1\nu(1-q)(d+\gamma)]}\,. \tag{5}$$

For p_c to be viable, the critical vaccination threshold must be bounded by zero and unity i.e., $0 \le p_c \le 1$. Note that since $1 - 1/\mathcal{R}_0 > 0$, $p_c > 0$ only when $(d+k_1+k_2)(d+\gamma_W) - Gk_1\nu(1-q)(d+\gamma) > 0$. If $q = 1$ or $G = 0$, $(d+k_1+k_2)(d+\gamma_W) - Gk_1\nu(1-q)(d+\gamma) = (d+k_1+k_2)(d+\gamma_W) > 0$. When $0 \le q < 1$ and $0 < G \le 1$, $(d+k_1+k_2)(d+\gamma_W) - Gk_1\nu(1-q)(d+\gamma) > 0$ when $\nu < (k_1+k_2+d)(d+\gamma_W)/(k_1G(1-q)(d+\gamma))$. However, we also see that $p_c > 0$ is guaranteed when $0 \le \nu \le 1$, that is, when W individuals are less susceptible to measles than S individuals (i.e., W individuals have some neutralizing immunity).

Observe that $p_c = 1 - 1/R_0$ when $k_1, k_2 = 0$. Also observe that p_c increases as G approaches unity, ν approaches unity, q approaches zero, or γ_W approaches γ. Finally, for $p_c < 1$, the following inequality must be true

$$\mathcal{R}_0 < \frac{(d+k_1)(d+k_2)(d+\gamma_W)}{k_1k_2(d+\gamma_W) + Gd\nu k_1(1-q)(d+\gamma)}\,. \tag{6}$$

We use Eq. (5) to investigate the region where p_c is viable. Figure 2 plots p_c as k_1 and k_2 vary, $\mathcal{R}_0 = [3, 5, 8, 10, 12, 16, 18]$, and assuming $G\nu(1-q) = [0.1, 0.5, 0.8]$ years^{-1} (left to right columns), $\gamma_W = [\gamma, 3\gamma, 5\gamma]$ (top to bottom rows), and $1/d = 83.33$ years. We observe that as $\mathcal{R}_0$, k_1 and k_2 decrease, the region where the critical vaccination threshold exists increases. However, as k_1 and k_2 increase, realistic values of p_c do not exist, even when the mean overall waning immunity time $1/k_1 + 1/k_2$ is greater than the average lifetime $1/d$. Finally, we see that as $G\nu(1-q)$ increases and γ_W approaches γ, p_c becomes less dependent on k_2.

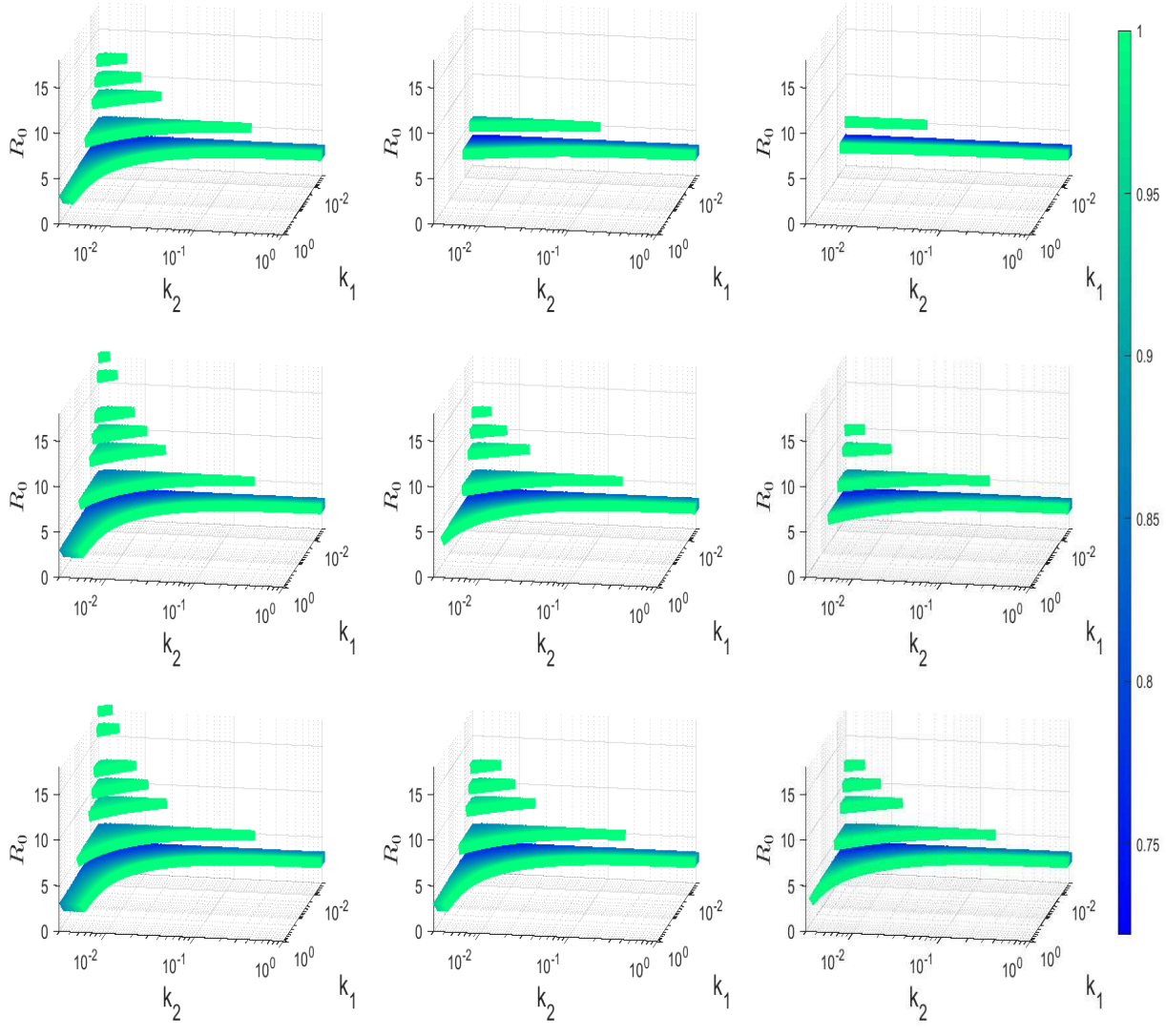


Figure 2: Critical vaccination threshold p_c (colourbar) for different values of $\mathcal{R}_0 = [4, 8, 12, 14, 16, 18, 20]$, k_1 and k_2, when $\gamma_W = [\gamma, 3\gamma, 5\gamma]$ (top to bottom row), $d = 1/78$ years^{-1}, $G = 1$, $\nu(1-q) = (0.1, 0.5, 0.8)$ (left to right panels). k_1 and k_2 are shown in log-scale.

4.4 Probability of no measles transmission

Upon importation of a measles infected into a vaccinated population, the infected may or may not transmit the infection to others. Given an importation, the probability of no new infections is

$$\begin{aligned} Prob_{no\,outbreak} &= Pr(I_0=1)\frac{\gamma+d}{\gamma+d+\beta S_0+\beta\nu(1-q)W_0} + Pr(I_{W,0}=1)\frac{\gamma_W+d}{\gamma_W+d+\beta G S_0+\beta G\nu(1-q)W_0} \\ &= Pr(I_0=1)\frac{1}{1+\mathcal{R}_{0,I\to I}+\mathcal{R}_{0,I\to I_W}} + Pr(I_{W,0}=1)\frac{1}{1+\mathcal{R}_{0,I_W\to I}+\mathcal{R}_{0,I_W\to I_W}} \end{aligned} \tag{7}$$

where $Pr(I_0=1)$ and $Pr(I_{W,0}=1)$ are the probabilities that the initial infected is an I or I_W individual, respectively, and $\mathcal{R}_{0,A\to B}$ are the type reproduction numbers where an A infected makes a B infected and $A,B=\{I,I_W\}$ (see Appendix for derivation of type reproduction numbers). Note that as the type reproduction numbers increase, the probability of no measles outbreak decreases. Also observe that the probability of no measles outbreak is given by $1/(1+\mathcal{R}_{0,I\to I}) = 1/(1+\mathcal{R}_0)$ when there is no waning immunity in vaccinated individuals.

4.5 Probability of a measles outbreak

The probability of a measles outbreak of at least one infection is given by

$$Prob_{outbreak} = 1 - Prob_{no\,outbreak}\,. \tag{8}$$

4.6 Final Size of an Outbreak

When $Prob_{outbreak} > 0$, the total number of infections can be determined from the final size equation. Using the method outlined in [23], and ignoring demographics ($\lambda, d = 0$), System (1) has an outbreak final size of

$$\begin{aligned} \ln\left(\frac{S_0}{S_\infty}\right) &= \frac{\beta}{\gamma+d}(S_0-S_\infty) + \frac{\beta G(1-q)}{\gamma_W+d}(W_0-W_\infty) + \frac{\beta}{\gamma+d}I_0 + \frac{\beta G}{\gamma_W+d}I_{W,0} \\ W_\infty &= W_0\left(\frac{S_\infty}{S_0}\right)^\nu \end{aligned} \tag{9}$$

where I_0 and $I_{W,0}$ are the initial numbers of I and I_W infecteds, S_0 and W_0 are determined from the DFE (with demographics, i.e., $\lambda, d \neq 0$), and S_∞ and W_∞ are the sizes of the S and W populations when the outbreak has concluded ($S_\infty < S_0$ and $W_\infty < W_0$). Rewriting Eq. (9) in terms of $\mathcal{R}_0$ and the number of S and W individuals that were infected and recovered i.e., $R_{S,\infty} = S_0 - S_\infty$, $R_{W,\infty} = W_0 - W_\infty$, we have

$$\begin{aligned} \ln\left(\frac{S_0}{S_0-R_{S,\infty}}\right) &= \frac{\mathcal{R}_0}{N}\left(R_{S,\infty} + \frac{\gamma+d}{\gamma_W+d}G(1-q)R_{W,\infty} + I_0 + \frac{\gamma+d}{\gamma_W+d}GI_{W,0}\right) \\ R_{W,\infty} &= W_0\left(1-\left(1-\frac{R_{S,\infty}}{S_0}\right)^\nu\right)\,. \end{aligned} \tag{10}$$

4.7 Measles in Ontario, Canada

Ontario, Canada recently experienced measles outbreaks in various regions of the province, with the largest in the Southwestern Ontario Public Health Region (SOPHR). We will now employ the tools developed here to study the SOPHR measles epidemic.

SOPHR has a resident population of 216,533 with 23.8%, 56.0% and 20.2% in groups aged 0-19 years, 20-64 years, and >65 years, respectively [24]. The first confirmed measles case in SOPHR was reported

in November 2025. As of August 12, 2025, there were 769 confirmed measles cases and the epidemic was in decline [25]. According to an earlier report, 74% of SOPHR confirmed cases were in ages $\leq$18 years and 88.8% were in unimmunized individuals [26]. In studies across Canada, seroprevalence has been documented to be 78-92% in predominantly vaccinated populations (younger age groups) and 95-99% in older age groups that are assumed to have gained immunity from infection [27, 28]. In a recent review, a median R_0 value of 15.3 in the Americas was estimated [16].

Denote θ to be the vector of parameters required to simulate the model and let D be reported measles characteristics in SOPHR, Ontario, and Canada from the literature discussed above. Through Latin Hypercube Sampling (LHS), we generate 100,000 parameter sets, θ, taken from plausible ranges of all model parameters in Table 1. Using these parameter sets and assuming $Pr(I_0 = 1) = Pr(I_{W,0} = 1) = 0.5$, we find S_0, V_0, W_0, β, $\mathcal{R}_c$, S_∞, and W_∞, and simulate the model (ignoring demographics) to determine the measles epidemic peak size and time. Over all parameter sets, we find 695 sets to have epidemic final sizes $R_\infty + R_{W,\infty}$ greater than 770 and less than 2000 total infections. Considering epidemic final size upper bounds of 1500 or 1000 total infections, this reduces to 416 and 152 parameter sets, respectively. Table 2 lists the mean (standard deviation), minimum and maximum of the model parameters and their corresponding results for the $\leq$ 2000, 1500, and 1000 total infection scenarios. The results indicate a vaccination uptake of $\approx$ 86%, basic and control reproduction numbers of $\approx$ 12.3 and 2.7, and mean waning rates of 0.009 and 0.007 years^{-1}, corresponding to immunity half-lives of 77 years from V to W and 99 years from W to S. We also find that W individuals are 55% less susceptible than S individuals (ν), newly exposed W individuals have a 43% probability of experiencing an infection rather than a boost in immunity (q), and I_W individuals are 52% less infectious than their I counterparts (G). Finally, we find that the epidemic peak occurs $\approx$ 0.27 years (3.24 months) after epidemic commencement, the epidemic peak does not exceed 300 infections, the SOPHR subpopulation involved in the outbreak, N_0, ranges from 4,400 to 6,500 individuals, and $\approx$ 77% of all infections ($R_{S,\infty}/(R_{S,\infty} + R_{W,\infty})$ are in the fully susceptible class S.

It is of interest to explore the measles outbreak when vaccine uptake lies at the lower and upper bounds of 78% and 92% [27, 28]. Model results are listed in Table 3 using 100,000 parameter sets. Notably, we find that only 210 parameter sets have final sizes between 770 and 2000 when vaccine uptake is 78%, but this increases to 2371 parameter sets when vaccine uptake is 92%. Comparing the two scenarios, R_0 and R_c are higher when vaccine coverage is 92%, and the total number of people involved in the outbreak ($N_0 = S_0 + W_0 + V_0$) and final size of the outbreak ($R_{S,\infty} + R_{W,\infty}$) are smaller. Interestingly, we find a large difference in the waning rate of immunity from W to S (k_2) where the waning rate is 50% slower when vaccince uptake is 78%. Finally, we remark that the final size of the epidemic is higher and the outbreak peak magnitude is smaller when vaccine uptake is 78% and the peak time is 6 months ($0.792 - 0.298 = 0.494 years = 6 months$) later in time.

5 Discussion

Measles vaccine-induced immunity may wane [13]. In turn, individuals with waning vaccine-induced immunity may contract measles infection and contribute to the spread of measles. Considering this, to provide best-informed public health decision-making, new mathematical definitions of the control reproduction number, critical vaccination threshold, outbreak probability, and the final size of a measles outbreak must be determined.

We have determined that the current and very popular approximations of the control reproduction number, $\mathcal{R}_c = \mathcal{R}_0(1-p)$ and the critical vaccination threshold, $p_c = 1 - 1/\mathcal{R}_0$ provide lower bounds of the new definitions of $\mathcal{R}_c$ and p_c (Eq.'s (4) and (5)) when vaccine-indcued immunity is allowed to wane.

max R	2000	1500	1000
no. sims	695	416	152
p	0.864 (0.040, [0.781, 0.920])	0.864 (0.040, [0.781, 0.920])	0.864 (0.041, [0.781, 0.919])
$\mathcal{R}_0$	12.3 (5.8, [3.0, 27.0])	12.3 (5.9, [3.0, 27.0])	12.3 (6.0, [3.0, 27.0])
β	0.065 (0.042, [0.008, 0.269])	0.076 (0.046, [0.009, 0.269])	0.093 (0.055, [0.014, 0.269])
γ_W	78.6 (29.6, [26.1, 129.7])	76.7 (29.6, [26.1, 129.7])	75.3 (29.3, [26.3, 128.3])
G	0.515 (0.295, [0.001, 0.998])	0.522 (0.300, [0.002, 0.998])	0.518 (0.283, [0.012, 0.997])
ν	0.549 (0.263, [0.028, 0.999])	0.546 (0.266, [0.037, 0.997])	0.552 (0.277, [0.037, 0.997])
q	0.428 (0.245, [0.001, 0.947])	0.435 (0.244, [0.004, 0.947])	0.466 (0.249, [0.006, 0.906])
k_1	0.0085 (0.0055, [0.0004, 0.0200])	0.0087 (0.0056, [0.0004, 0.0199])	0.0091 (0.0057, [0.0004, 0.0199])
k_2	0.0073 (0.0055, [0.0000, 0.0199])	0.0073 (0.0056, [0.0000, 0.0199])	0.0065 (0.0054, [0.0000, 0.0197])
N_0	6492.6 (4106.2, [1288.6, 27510.1])	5325.7 (3346.2, [1288.6, 21531.6])	4408.1 (2978.6, [1288.6, 21531.6])
S_0	1341.3 (586.3, [364.3, 4166.2])	1101.9 (469.2, [364.3, 3306.3])	876.2 (369.0, [364.3, 2236.4])
W_0	1347.8 (1259.6, [140.1, 10905.7])	1126.8 (1088.9, [140.1, 9042.1])	987.1 (930.2, [140.1, 6900.0])
V_0	3803.4 (3159.4, [433.6, 23236.2])	3096.9 (2524.5, [433.6, 16867.6])	2544.8 (2243.6, [433.6, 15060.2])
$\mathcal{R}_c$	2.8 (1.1, [1.2, 5.0])	2.8 (1.1, [1.2, 5.0])	2.7 (1.1, [1.2, 4.9])
$R_{S,\infty}$	1042.7 (313.0, [357.9, 1753.6])	850.3 (205.4, [357.9, 1321.2])	652.4 (110.8, [357.9, 894.3])
$R_{W,\infty}$	321.1 (171.8, [79.1, 954.1])	257.3 (127.5, [79.1, 669.8])	198.8 (91.7, [79.1, 478.8])
peak size	290.2 (169.0, [28.9, 848.8])	235.7 (128.7, [28.9, 592.4])	171.9 (89.0, [28.9, 397.6])
peak time	0.271 (0.212, [0.077, 0.991])	0.266 (0.211, [0.077, 0.991])	0.276 (0.219, [0.077, 0.948])

Table 2: SOPHR measles epidemic summary table for different maximum final sizes $R = R_{S,\infty} + R_{W,\infty}$. Mean (std dev., [min, max]) values are reported for simulations with final size lower bound of 770 and upper bounds of 2000, 1500 and 1000 infections.

p	78%	92%
no. sims	210	2371
$\mathcal{R}_0$	4.9 (0.9, [3.1, 7.7])	14.4 (6.0, [3.0, 27.0])
β	0.011 (0.002, [0.007, 0.019])	0.061 (0.042, [0.008, 0.259])
γ_w	83.0 (27.9, [26.7, 129.7])	79.0 (29.8, [26.0, 129.9])
G	0.505 (0.287, [0.002, 0.990])	0.493 (0.286, [0.000, 0.999])
ν	0.586 (0.233, [0.043, 0.999])	0.524 (0.269, [0.016, 1.000])
q	0.432 (0.250, [0.003, 0.902])	0.448 (0.260, [0.000, 0.962])
k_1	0.0071 (0.0049, [0.0006, 0.0196])	0.0081 (0.0056, [0.0003, 0.0200])
k_2	0.0042 (0.0044, [0.0000, 0.0191])	0.0079 (0.0055, [0.0000, 0.0200])
N_0	11747.0 (1524.3, [10009.3, 17934.5])	8669.4 (5864.8, [1449.7, 38233.3])
S_0	3142.2 (498.1, [2220.1, 4457.3])	1362.2 (610.3, [382.8, 4099.8])
W_0	2451.7 (1432.6, [399.8, 6794.8])	1698.6 (1693.1, [133.0, 17954.1])
V_0	6153.1 (1643.4, [3266.2, 11762.2])	5608.6 (4795.8, [545.2, 32669.1])
$\mathcal{R}_c$	1.3 (0.1, [1.2, 1.8])	2.6 (1.1, [1.2, 5.0])
$R_{S,\infty}$	1400.8 (226.8, [798.6, 1770.5])	1022.5 (318.2, [380.0, 1776.1])
$R_{W,\infty}$	293.4 (132.6, [91.5, 848.7])	330.3 (176.0, [75.2, 979.6])
peak size	110.2 (41.7, [42.2, 266.0])	261.1 (154.4, [27.4, 813.9])
peak time	0.792 (0.149, [0.388, 0.999])	0.298 (0.221, [0.067, 0.999])

Table 3: SOPHR measles epidemic summary table when vaccine uptake is 78% and 92%. Mean (std dev., [min, max]) values are reported for simulations with final size lower bound of 770 and upper bound of 2000 infections.

Figure 2 shows that even very small rates of waning immunity can make vaccine-induced herd immunity impossible to achieve.

Measles outbreaks are not often observed in highly vaccinated populations. Eq. (7) confirms this. When the type reproduction numbers $\mathcal{R}_{0,I\to I_W}$, $\mathcal{R}_{0,I_W\to I}$ and $\mathcal{R}_{0,I_W\to I_W}$ decrease, for example, when W_0, ν, $(1-q)$, and G decrease, the probability of no measles outbreak increases.

At the beginning of an outbreak it is possible to estimate the expected number of infecteds over the entire outbreak. This can be done using the final size equations shown in Eq. (10). During or upon conclusion of an outbreak, these equations can also be used to estimate model parameters including the effective population that was involved in the outbreak ($N_0 = S_0 + W_0 + V_0$), the rates of waning immunity that the vaccinated population experiences (k_1, k_2), and how susceptible and infectious W individuals (individual with waning vaccine-induced immunity) are (i.e., G, ν, q).

We have applied the mathematical tools derived here to a measles outbreak in Southwestern Ontario (Table 2). Considering different maximum final sizes of 2000, 1500 or 1000 infections, we find consistency in vaccination uptake ($p \approx 86\%$) and the basic and control reproduction numbers ($\mathcal{R}_0 \approx 12.3$ and $\mathcal{R}_c \approx 2.8$). We also find consistency across model parameters associated with the susceptibility of W ($\nu \approx 0.55$), the probability of an infection rather than a boost in immunity ($q \approx 0.43$) and the infectiousness of I_W ($G \approx 0.52$). Interestingly, the waning rate of immunity from V to W, $k_1 \approx 0.009$, corresponds to a half-life of 77 years. A recent study by Bolotin et al. [13] showed that antibody immunity can decay over time in vaccinated individuals, whereby some susceptibility could be reached approximately 51 years after full immunization. Our result is thus similar in magnitude. Finally, we have estimated that the SOPHR subpopulation involved in the outbreak, N_0, ranges from 4,400 to 6,500 individuals, and that $\approx 77\%$ of all infections ($R_{S,\infty}/(R_{S,\infty} + R_{W,\infty})$ are in the fully susceptible class S. This is also similar in magnitude to what has been reported in the SOPHR measles outbreak – 88% of all reported cases (symptomatic and/or contact traced) lie in the unvaccinated population [26].

We have provided important updates to calculations that are commonly used to assess the risk and potential of a measles epidemic. The results of our study, however, can be improved. First, the current calculations (and the previous ones that we have updated here) are determined from models that assume that the population is well-mixed. Rather, there should be a contact network whereby individuals have many contacts with their friends, family and co-workers, but less with others in the population. Second, the models ignore age structure, but measles is a childhood infection, and the measles vaccine is provided in the childhood vaccination program. Finally, apart from our study of the probability of no new infections, the current model framework ignores stochastic effects throughout the outbreak. This renders any study of the variability in important public health measures such as the epidemic peak size, peak time, end time and final size infeasible. Stochastic contact- and age-structured models represent courses for future work.

6 Declarations

6.1 Ethics approval and consent top participate

Not applicable

6.2 Consent for publication

Not applicable

6.3 Availability of data and materials

The datasets generated and/or analyzed during the current study are available in the Measles Waning - BMC Public Health repository, https://www.dropbox.com/scl/fo/5c6ysikxz3mt5ztstnmg8/AL1gI2xpHyw6rNd8jGdu2IU?rlkey=7aub4otvsevb03bjizwopq1x0&st=471rmi3a&dl=0.

6.4 Competing interests

The authors declare that they have no competing interests.

6.5 Funding

JMH is supported by the Natural Sciences and Engineering Research Council of Canada Discovery Grant program (NSERC DG) and the York University Research Program.

6.6 Authors' contributions

JMH conceived of the study. MR, EA, ST and JMH developed the study, conducted analysis, wrote the main manuscript and prepared figures. All authors reviewed the manuscript.

6.7 Acknowledgments

We thank Shelly Bolotin and Natasha Crowcroft for helpful discussions.

Appendix

Type Reproduction Numbers

Infected individuals in I and I_w can transmit infection to susceptibles S and individuals with waning immunity W. We are interested in quantifying the type reproduction numbers $R_{0,A\to B}$, $A, B \in \{I, I_w\}$, defined as the expected number of new infections of type $B \in \{I, I_w\}$ caused by a single infectious individual of type $A \in \{I, I_w\}$ in a population of susceptibles (fully susceptible, S; partially susceptible W). These expressions are derived under the assumption that the epidemic is in its initial phase, so that S_0 and W_0 are constant (at the DFE) and the system dynamics can be approximated by a branching process. The terms incorporate heterogeneity in susceptibility and infectiousness: individuals with waned immunity W are less susceptible (scaled by $\nu(1-q)$), and infected individuals with waned immunity I_w may transmit at a reduced rate (scaled by G). The reproduction numbers are given by:

	To I	To I_w
From I	$\mathcal{R}_{0,I\to I} = \dfrac{\beta S_0}{\gamma}$	$\mathcal{R}_{0,I\to I_w} = \dfrac{\beta\nu(1-q)W_0}{\gamma}$
From I_w	$\mathcal{R}_{0,I_w\to I} = \dfrac{\beta G S_0}{\gamma_w}$	$\mathcal{R}_{0,I_w\to I_w} = \dfrac{\beta G\nu(1-q)W_0}{\gamma_w}$

We note that each type reproduction number is given by the product of (1) the duration of infection of the infectious individual ($1/\gamma or 1/\gamma_w$), (2) the infectiousness of the infectious individual ($\beta or G\beta$), (3) the magnitude of the susceptible populations at the DFE (S_0 and W_0), (4) the susceptibility of individuals with waned immunity W ($1, \nu$), (5) and the probability that the newly exposed contact becomes and infected (1 or $(1-q)$). The components of all type reproduction numbers are given in Table 4.

Type Reproduction Number	Infectious Individual	Infection Duration	Infectiousness	Susceptible Population Magnitude	Susceptibility	Probability of Becoming an Infected
$\mathcal{R}_{0,I\to I}$	I	$1/\gamma$	β	S_0	1	1
$\mathcal{R}_{0,I\to I_w}$	I	$1/\gamma$	β	W_0	ν	$1-q$
$\mathcal{R}_{0,I_w\to I}$	I_w	$1/\gamma_w$	βG	S_0	1	1
$\mathcal{R}_{0,I_w\to I_w}$	I_w	$1/\gamma_w$	βG	W_0	ν	$1-q$

Table 4: Type Reproduction Numbers: Derivation

References

[1] MJ Keeling and P Rohani. *Modeling infectious diseases in humans and animals*. Princeton University Press, 2008.

[2] WJ Moss and DE Griffin. Global measles elimination. *Nature Reviews Microbiology*, 4(12):900–908, 2006.

[3] World Health Organization. Measles. https://www.who.int/health-topics/measles#tab=tab_1. Accessed: 2025-09-18.

[4] World Health Organization (WHO). https://www.who.int/immunization/diseases/measles/en/. Accessed: 2025-09-18.

[5] Public Health Agency of Canada. Measles vaccine: Canadian immunization guide. https://www.canada.ca/en/public-health/services/publications/healthy-living/canadian-immunization-guide-part-4-active-vaccines/page-12-measles-vaccine.html#p4c11a4. Accessed: 2025-09-18.

[6] A Pillsbury and H Quinn. An assessment of measles vaccine effectiveness, Australia, 2006-2012. *Western Pacific Surveillance and Response Journal*, 6:43–50, 2015.

[7] Centers for Disease Control and Prevention (CDC). Measles vaccination. https://www.cdc.gov/vaccines/vpd/mmr/public/index.html. Accessed: 2025-09-18.

[8] Government of Canada. Measles and rubella weekly monitoring report. https://health-infobase.canada.ca/measles-rubella/. Accessed: 2025-09-18.

[9] Government of Canada. Vaccination coverage in canada. https://www.canada.ca/en/public-health/services/immunization-vaccines/vaccination-coverage.html. Accessed: 2025-09-18.

[10] AO Faneye, JA Adeniji, BA Olusola, BO Motayo, and GB Akintunde. Measles virus infection among vaccinated and unvaccinated children in nigeria. *Viral Immunol*, 6, 2015.

[11] E Avramovich, V Indenbaum, M Haber, Z Amitai, E Tsifanski, S Farjun, A Sarig, A Bracha, K Castillo, MP Markovich, and I Galor. Measles outbreak in a highly vaccinated population - israel, july-august 2017. *MMWR Morb Mortal Wkly Rep*, 42:1186–1188, 2018.

[12] N López Perea, A Fernández-García, JE Echevarría, F de Ory, M Pérez-Olmeda, and J Masa-Calles. Measles in vaccinated people: Epidemiology and challenges in surveillance and diagnosis in the post-elimination phase. spain, 2014-2020. *Viruses*, 10, 2021.

[13] S Bolotin, S Osman, SL Hughes, A Ariyarajah, AC Tricco, S Khan, L Li, C Johnson, L Friedman, N Gul, R Jardine, M Faulkner, SJM Hahné, JM Heffernan, A Dabbagh, PA Rota, A Severini, M Jit, DN Durrheim, WA Orenstein, WJ Moss, S Funk, N Turner, W Schluter, JS Jawad, and NS Crowcroft. In elimination settings, measles antibodies wane after vaccination but not after infection: A systematic review and meta-analysis. *J Infect Dis*, 226:1127–1139, 2022.

[14] O Diekmann, H Heesterbeek, and H Britton. *Mathematical Tools for Understanding Infectious Disease Dynamics*. Princeton University Press, 2013.

[15] JM Heffernan, RJ Smith?, and LM Wahl. Perspectives on the basic reproductive ratio. *J.R.Soc. Interface*, 2:281–293, 2005.

[16] FM Guerra, S Bolotin, G Lim, J Heffernan, SL Deeks, Y Li, and NS Crowcroft. The basic reproduction number (R0) of measles: a systematic review. *The Lancet Infectious Diseases*, 17(12):e420 – e428, 2017.

[17] R-M Carlsson, LM Childs, Z Feng, JW Glasser, JM Heffernan, J Li, and G Röst. Modeling the waning and boosting of immunity from infection or vaccination. *Journal of Theoretical Biology*, 497:110265, 2020.

[18] JS Lavine, AA King, and ON Bjørnstad. Natural immune boosting in pertussis dynamics and the potential for long-term vaccine failure. *Proceedings of the National Academy of Sciences*, 108(17):7259–7264, 2011.

[19] MP Dafilis, F Frascoli, J McVernon, JM Heffernan, and JM McCaw. The dynamical consequences of seasonal forcing, immune boosting and demographic change in a model of disease transmission. *Journal of Theoretical Biology*, 361:124–132, 2014.

[20] MP Dafilis, F Frascoli, J McVernon, JM Heffernan, and JM McCaw. Dynamical crises, multistability and the influence of the duration of immunity in a seasonally-forced model of disease transmission. *Theoretical Biology and Medical Modelling*, 11(1):1–10, 2014.

[21] World Health Organization (WHO). Data overview for Canada. http://www.who.int/countries/can/en/. Accessed: 2025-09-18.

[22] World Health Organization (WHO). Measles. http://www.who.int/news-room/fact-sheets/detail/measles. Accessed: 2018-08-14.

[23] J Arino, F Brauer, P van den Driessche, J Watmough, and J Wu. A final size relation for epidemic models. *Mathematical Biosciences & Engineering*, 4(2):159–175, 2007.

[24] Southwestern Public Health. Community profile. https://www.swpublichealth.ca/media/qsqjrhtf/rep-202408-community-profile-report.pdf. Accessed: 2025-09-18.

[25] Public Health Ontario (PHO). Enhanced epidemiology summary: Measles in ontario. https://www.publichealthontario.ca/-/media/Documents/M/24/measles-ontario-epi-summary.pdf. Accessed: 2025-09-18.

[26] Southwestern Public Health. Soutwestern public health measles outbreak report. https://www.swpublichealth.ca/media/1qwek0fe/measles-outbreak-report_june-12-2025.pdf. Accessed: 2025-09-18.

[27] S Bolotin, A Severini, T Hatchette, E McLachlan, R Savage, SL Hughes, J Wang, SL Deeks, S Wilson, M Brisson, et al. Assessment of population immunity to measles in ontario, canada: a canadian immunization research network (cirn) study. *Human Vaccines & Immunotherapeutics*, 15(12):2856–2864, 2019.

[28] S Osman, N Crowcroft, E McLachlan, T Hatchette, C Perez-Iratxeta, E Joh, J Wright, SA Halperin, S Deeks, S Wilson, et al. Population immunity to measles in canada using canadian health measures survey data–a canadian immunization research network (cirn) study. *Vaccine*, 40(23):3228–3235, 2022.